Electronic structure of the Ge(111)-$c(2\times8)$ surface

J. Aarts, A. J. Hoeven, and P. K. Larsen
Philips Research Laboratories, P.O. Box 80 000, NL-5600 JA Eindhoven, The Netherlands
(Received 9 July 1987; revised manuscript received 9 November 1987)

Angularly resolved photoemission measurements were performed on Ge(111)-$c(2\times8)$ surfaces which were prepared by molecular-beam epitaxy. The spectra allow a detailed determination of the dispersions of the four surface states which were found. This description differs in important respects from previously published surface band dispersions. The results can partly be explained by the presence of adatoms on the reconstructed surface.

I. INTRODUCTION

The study of the electronic band structure of semiconductors is of continuing interest in order to provide links between the atomic structure and the electronic properties of the surface. Such studies are even gaining in significance since, due to the advent of the scanning tunneling microscope (STM), it is becoming possible to map the electronic states onto the surface in real space.[1]

The annealed Ge(111) surface possesses a reconstruction described by a $c(2\times8)$ unit cell, which is too large to lend itself to band-structure calculations. Earlier angularly resolved photoemission studies reported the existence of at least two surface states at about 0.8 and 1.4 eV below the top of the valence band.[2–4] The energy dispersions as a function of electron momentum parallel to the surface $k_{\parallel}$ do not, however, show the periodicity of the large unit cell, but rather correspond to a (1×1) surface cell,[2] or possibly a (2×2) surface cell.[3,4] This may not be considered surprising as photoemission is known to be sensitive to the short-range order on the surface; also, a recent STM study of the Ge(111)-$c(2\times8)$ surface revealed that the $c(2\times8)$ structure is built from (2×2) and $c(4\times2)$ subunits which are also present as separate entities.[5] Band-structure calculations for such units are more feasible and have already been performed for similar possible subunits on the Si(111)-(7×7) surface.[6]

Apart from the fact that it therefore seems possible to compare theory and experiment for the Ge(111) surface, the experimental facts themselves are not entirely clear. Nicholls *et al.*, measuring with photon energies around 10 eV, found new surface states[7] in addition to the two states mentioned above. On the other hand Bringans *et al.*,[4] measuring with photon energies around 20 eV, were not able to confirm these findings. In this study we present measurements at photon energies of 19, 23, and 36 eV on Ge(111) surfaces which have been prepared *in situ* by molecular-beam epitaxy (MBE). The results from measurements at photon energies of 19 and 23 eV show the presence of four different surface states. Three of these can be identified around the Γ point of the surface Brillouin zone. This has not been reported before. A detailed description of the dispersions of all four states presents a rather different picture from previously published results and we shall discuss the possible origins for the present findings. It will also be shown that the preparation of the surface plays a crucial role in obtaining spectra with features sharp enough to identify all the surface states present.

II. EXPERIMENT

The experiments were carried out using a vacuum chamber equipped with an electron-energy analyzer, a Knudsen cell for MBE growth of Ge, and a facility for surface characterization by reflection high-energy electron diffraction (RHEED). The base pressure of the cryo- and ion-pumped system was about 2×10^{-10} torr. This system was attached to the toroidal-grating monochromator of the A61 beam line at the ACO storage ring [Laboratoire pour l'Utilisation du Rayonnement Electromagnétique (LURE), Orsay, France].[8] Measurements were performed at photon energies of 19, 23 and 36 eV. Except when noted, the angle of incidence ϑ_i of the incident radiation with respect to the surface plane was 45°. The radiation is about 70% polarized and therefore the main component of the polarization vector (which is normal to the propagation direction in the plane containing the surface normal) also made an angle of 45° with respect to the surface plane. Electron energies were analyzed using a HAC-50 hemispherical analyzer from Vacuum Science Workshop (Manchester, UK) equipped with a four-element lens and at the exit plane a position-sensitive detection system. This consists of two channel plates for amplification and a resistive anode for detection. The principle of this method, which employs pulse-shape analysis, has been described by Wiza.[9] The decoding of the positional information from the resistive anode was performed by Canberra electronics in a configuration as described in Ref. 10. The combined resolution of monochromator and analyzer was about 150 meV at photon energies of 19 and 23 eV and about 250 meV at 36 eV. The detection angle ϑ_p of the electron emission could be varied by rotating the analyzer and is measured with respect to the surface normal. The angular resolution proved to be better than 1°. In the rest of the paper binding energies will be given relative to the top of the bulk valence bands E_{VBM} (VBM denotes

 ©1988 The American Physical Society

valence-band maximum); this level was determined by measuring the kinetic energy of electrons emitted from the Ge $3d_{5/2}$ core level with a photon energy of 40 eV and using a value of 29.35 eV for the Ge $3d_{5/2}$ binding energy.[11]

III. RESULTS

A. Surface preparation

Surface preparation was performed by growing a buffer layer of Ge on a clean Ge(111) surface at a growth temperature of about 550 °C. After cooling the substrate to 20 °C a sharp RHEED pattern was always found, showing the three domains of the $c(2\times8)$ structure and including the $\frac{1}{4}$-order spots which are usually not seen in low-energy electron diffraction (LEED) experiments.[12] An example of such a pattern, taken with the electron beam along a $\langle 2\bar{1}\bar{1}\rangle$ direction, is given in Fig. 1(a). It may be compared to the calculated three-domain $c(2\times8)$ pattern given in Fig. 1(b). To facilitate the comparison, Fig. 1(c) shows the effect of the elongation of the relevant

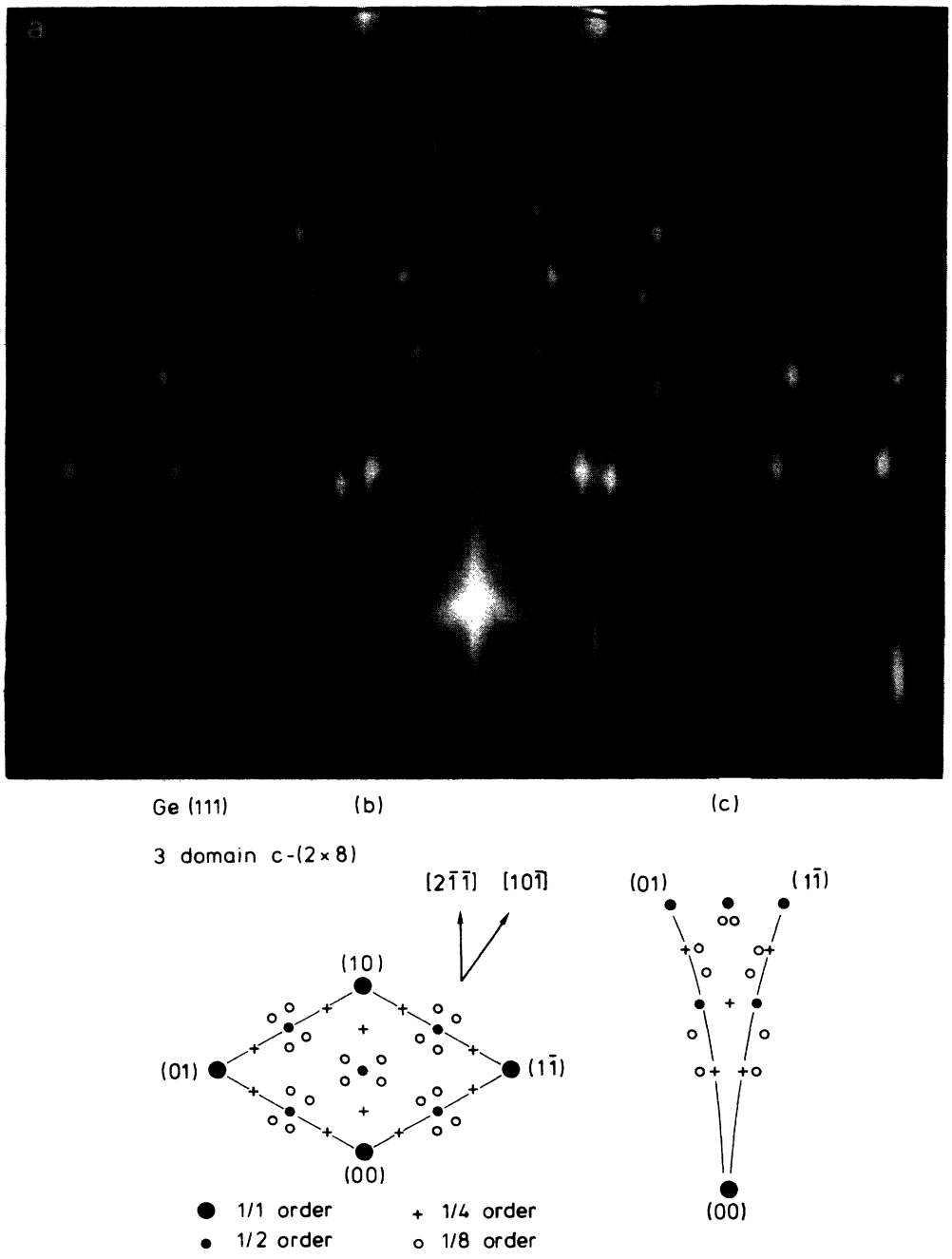

FIG. 1. (a) RHEED pattern of the three-domain $c(2\times8)$ reconstruction on a clean Ge(111) surface along a $\langle\bar{2}11\rangle$ azimuth. The electron-beam energy is 12 keV and the angle of incidence with respect to the surface plane 2.5°. (b) Reciprocal mesh for the three domains of the $c(2\times8)$ unit cell. (c) Elongation of the lower half of the pattern shown in (b) due to the RHEED geometry.

part of the pattern due to the usual RHEED geometry. It was found, however, that valence-band spectra taken directly after growth were not yet of high quality: the sharpness and intensity of the features could be increased considerably by annealing the sample for several hours at about 550 °C. This is shown in Fig. 2, where spectra are displayed which were measured with a photon energy of 23 eV and near-normal emission (emission angle $-2°$ along the $\langle 01\bar{1}\rangle$ azimuth). Due to a small amount of second-order radiation ($h\nu=46$ eV) a double-peaked structure, the Ge $3d$ core level (with binding energy 29.5 eV), can be seen at an apparent binding energy of about 6.5 eV (the binding energy is taken to be the negative of the initial energy). Since this structure should not be directly affected by the condition of the surface, the spectra in Fig. 2 are normalized to the right-hand peak of the doublet. Comparing the spectra taken directly after growth [Fig. 2(a)] and after annealing for about 20 min at 550 °C [Fig. 2(b)], it can be seen that the emission intensity of the peaks at low binding energy (comprising both bulk and surface features, as will be shown below) has increased by almost a factor of 2. Annealing for about 2 h at the same temperature [Fig. 2(c)] did not increase the emission intensity, but the features still became sharper. This can also be seen from the feature at a binding energy of 3.4 eV which has now become clearly visible. At the same time, visual inspection of the RHEED pattern did not show much difference, although some intensity increase of the diffraction spots may have been present.

We assume that the difference in appreciation of the surface quality found with RHEED and with photoemission is due to the different sampling areas of both techniques. The RHEED technique probes a coherent area which is in our case (depending on electron-beam divergence and angle of incidence) of the order of 100 Å in a direction perpendicular to the beam and a few thousand Å along the beam. The photoemission experiment probes an area of the order of the width of the electron wave functions, which is a few atomic distances. It appears, therefore, that some order already exists on the surface immediately after growth, but that it is not yet optimal; this is then improved by annealing.

B. Measurements along a $\langle 01\bar{1}\rangle$ azimuth

In Fig. 3 a series of spectra is shown, recorded at a photon energy of 23 eV for different values of the emission angle ϑ_p along a $\langle 01\bar{1}\rangle$ azimuth. This is equivalent to different values of $k_\parallel$ directed along the $\langle 01\bar{1}\rangle$ azimuth. The geometry of the surface reciprocal lattice and the (1×1) surface Brillouin zone is shown in Fig. 4. The spectra are chosen so as to give a good representation of the dispersions of bulk and surface states. They clearly show many details and in most of them at least six

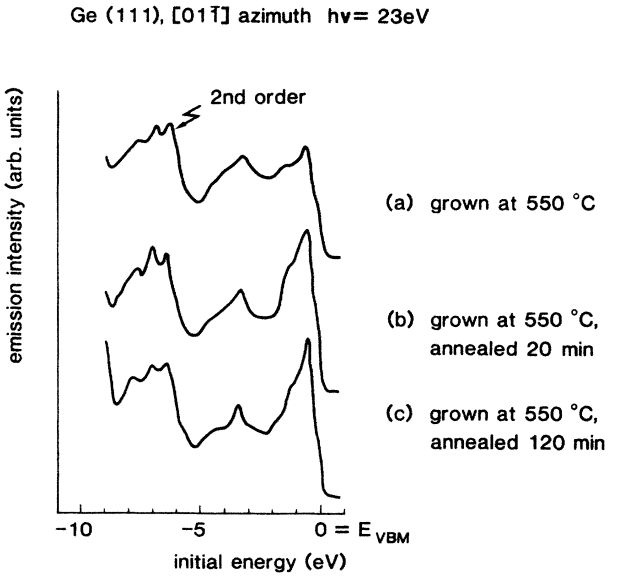

FIG. 2. Photoemission spectra recorded at a photon energy of 23 eV and an emission angle of $-2°$ along the $\langle 01\bar{1}\rangle$ azimuth. The core-level structure due to radiation of 46 eV has been labeled "2nd order." (a) Directly after growth at 550 °C. (b) Grown at 550 °C and annealed at 550 °C for 20 min. (c) Grown at 550 °C and annealed at 550 °C for 120 min.

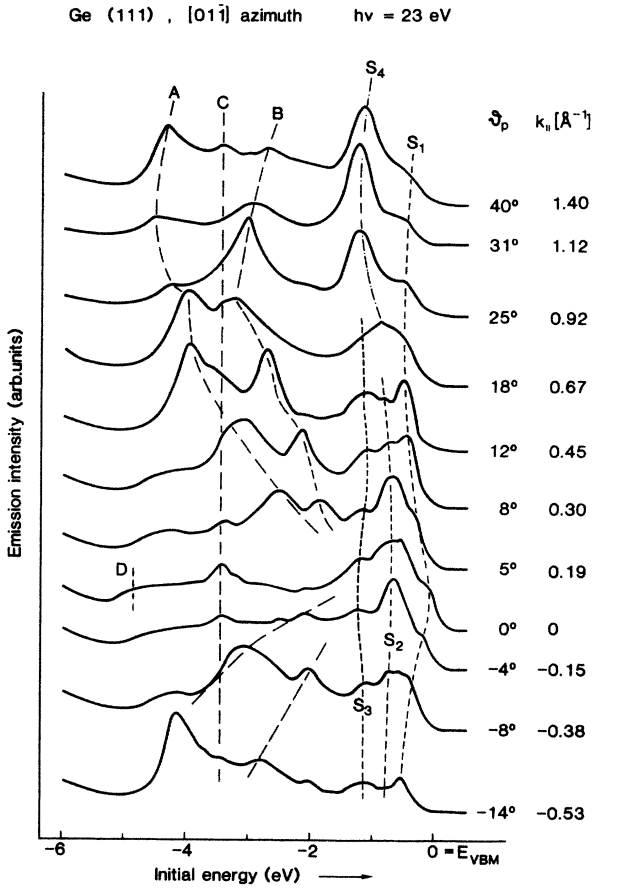

FIG. 3. Photoemission spectra recorded at a photon energy of 23 eV for various emission angles along a $\langle 01\bar{1}\rangle$ direction. Dashed lines serve as a guide to the eye. The values for $k_\parallel$ are calculated for a binding energy of 1 eV.

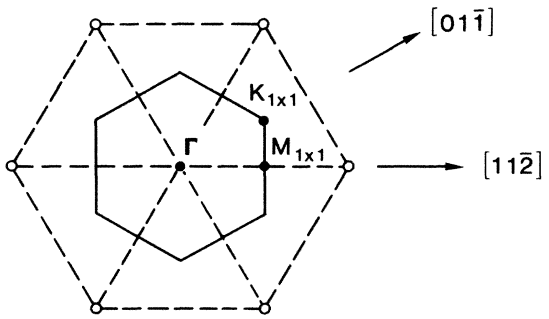

FIG. 4. Surface reciprocal unit mesh (dotted lines) and (1×1) surface Brillouin zone for the Ge(111) surface. The main symmetry points and directions are indicated.

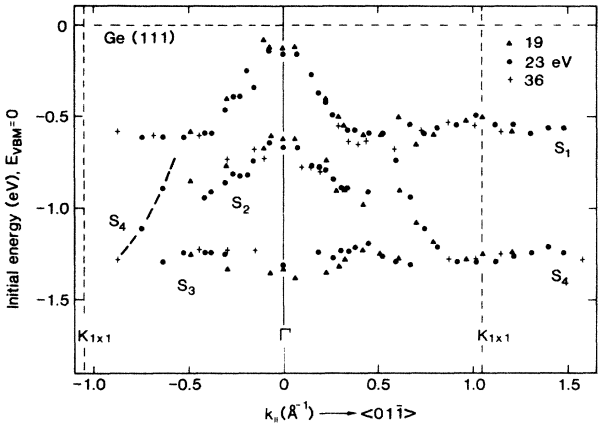

FIG. 5. Energy dispersions for the structures S_1-S_4 of Fig. 2 recorded at 23 eV. Also given are results from measurements at 19 and 36 eV.

features can be seen. Two of these, marked A and B, can be assigned to bulk band transitions.[13] They show strong dispersion as a function of $k_{\parallel}$. For normal emission, the binding energy of these transitions lies around 1–2 eV and the assignment of surface states around these emission angles is obviously difficult. The feature marked C shows no dispersion and lies at a binding energy of about 3.4 eV.

Comparing our data with results published earlier, it appears that the latter feature is at least related to the surface structure: it has been seen repeatedly in measurements performed on $c(2\times8)$ surfaces,[3,14] while it is conspicuously absent in measurements performed on cleaved surfaces. On $c(2\times8)$ surfaces it is present at the same binding energy for photon energies ranging from 17 to 45 eV,[14–16] although between 19 and 22 eV the feature is partly masked by a bulk band transition. In normal emission this transition is centered around a binding energy of 3 eV at a photon energy of 19 eV, and around 4 eV at 22 eV; in the normal-emission spectrum taken at 23 eV in Fig. 3 it is the shoulder around 5 eV marked D. At the photon energy of 21.2 eV, the bulk band transition and feature C are just separable, and take the form of a split peak (see the spectra in Ref. 3).

In the energy range between E_{VBM} and 2 eV, four structures can be discerned which are marked S_1-S_4. In Fig. 5 the energy dispersions of these states have been plotted as a function of $k_{\parallel}$, also using the data from measurements at 19 and 36 eV. The two states S_2 and S_3 with binding energies around 0.65 and 1.35 eV correspond to the two states observed in earlier studies as mentioned in the Introduction. Both states show clear energy dispersions; halfway in the Brillouin zone S_2 has dispersed to 0.9 eV, while S_3 has increased to 1.2 eV and is decreasing again.

In the spectra of Fig. 3 a clear shoulder is also present around normal emission with a binding energy of about 0.15 eV. With increasing polar angle this state grows in intensity and becomes a distinct peak around $\vartheta_p=8°$ ($k_{\parallel}\sim0.30$ Å^{-1}). At this point in the Brillouin zone the three features S_1-S_3 can be clearly and separately discerned. While S_1 increases in intensity and shifts to a binding energy of about 0.6 eV, S_2 decreases in intensity and can no longer be found beyond $\vartheta_p=14°$ ($k_{\parallel}\sim0.5$ Å^{-1}). In order to illustrate these changes a number of spectra are shown in Fig. 6 in somewhat more detail. At higher emission angles the state S_1 dwindles into a shoulder again but can be followed beyond the $K_{1\times1}$ point.

Around $\vartheta_p=16°$ a difficulty arises in the assignments of the peaks. This is most clearly visible in the spectra taken at 23 eV shown in Fig. 7. The peak at highest binding energy in the spectrum at 16° lies too low to be assigned to S_1 and too high for S_2. We believe this to be a different feature, S_4, which then disperses rapidly down to 1.25 eV with increasing ϑ_p. Note that for negative $k_{\parallel}$

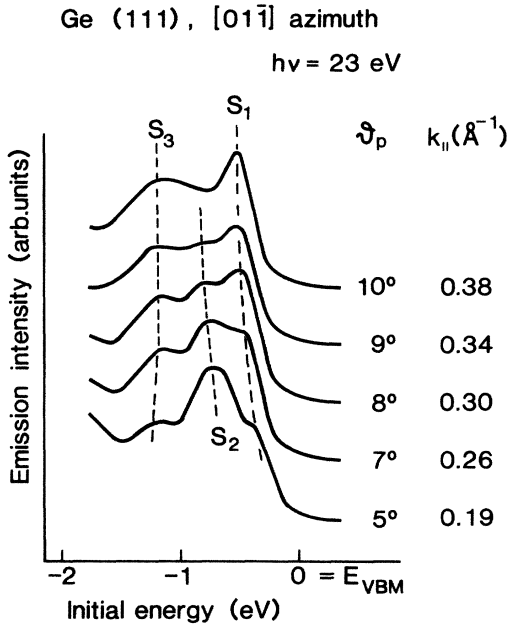

FIG. 6. Detailed evolution of the surface states S_1, S_2, and S_3 for emission angles between 5° and 10° along a ⟨01$\bar{1}$⟩ azimuth. Dashed lines serve as a guide to the eye. Values of $k_{\parallel}$ are calculated for a binding energy of 1 eV.

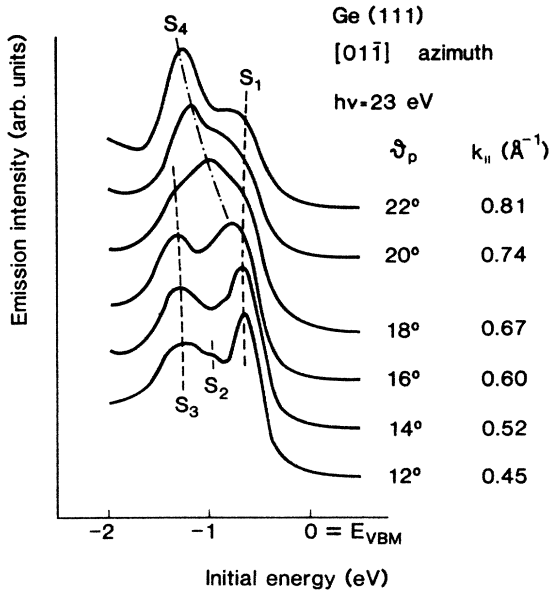

FIG. 7. Detailed evolution of the surface states S_1, S_3, and S_4 for emission angles between 14° and 22° along a $\langle 01\bar{1} \rangle$ azimuth. Dashed lines serve as a guide to the eye. Values of $k_{\parallel}$ are calculated for a binding energy of 1 eV.

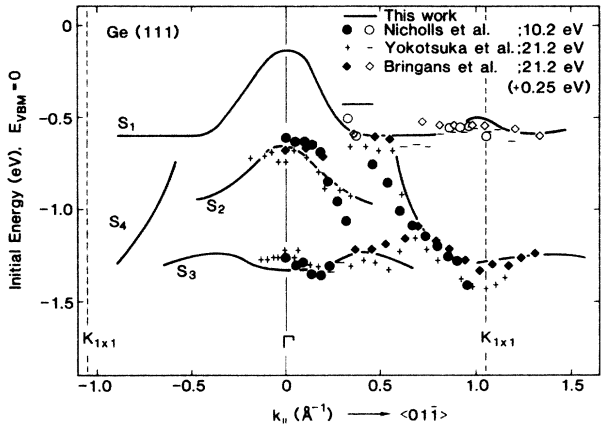

FIG. 8. Energy dispersions given in Fig. 5 (solid lines) compared with data from Nicholls *et al.* (Ref. 5), Yokotsuka *et al.* (Ref. 3), and Bringans *et al.* (Ref. 4).

some points were found that may also belong to S_4 (connected with a dashed line in Fig. 3) since they are found in a position mirrored with respect to Γ. Note also that the spectra in Fig. 7 do not give reason to believe that state S_3 actually disappears beyond $\vartheta_p = 18°$. Rather, it appears that around the $K_{1\times1}$ point the observed peak is a superposition of states S_3 and S_4. We shall come back to this point in the Discussion.

Four different states can therefore be identified in the emission spectra and it seems useful to compare these findings with the literature. Figure 8 shows the dispersions found in this work as solid lines, together with data from Nicholls *et al.* (Ref. 7) taken at 10.2 eV, from Yokotsuka *et al.* (Ref. 3) taken at 21.2 eV, and from Bringans *et al.* (Ref. 4) taken at 21.2 eV. In the comparison of the data a difference of 0.15 eV was assumed between E_{VBM} and the Fermi level E_F; the data of Bringans *et al.* were shifted by 0.25 eV to obtain better overall agreement. The diagram shows clearly that not only do no large discrepancies exist between the different measurements, but also why different dispersions were reported. The data agree particularly well with those of Nicholls *et al.*[7] Our measurements at 19 and 23 eV show that the highest-lying state S_1 is not only found around the $K_{1\times1}$ point, but can be followed from $K_{1\times1}$ to Γ. The measurements also agree with the data of Yokotsuka *et al.*,[3] who observed a structure with three separate peaks for one emission angle. We find that the three states S_1–S_3 are separately observable in a small range around $k_{\parallel} = 0.3$ Å^{-1}. In view of Fig. 8 it is not surprising that Bringans *et al.* decided on the presence of only two surface states. Both a good angular resolution ($\Delta k_{\parallel} \sim 0.04$ Å^{-1}) and good energy resolution ($\Delta E \sim 0.15$ eV) are needed to follow the evolution of the different states. If this is not the case, the states S_2 and S_3 around Γ and the states S_1 and S_4 around $K_{1\times1}$ emerge as two states. This is also the case for our own data measured at a photon energy of 36 eV and shown in the energy dispersion plot in Fig. 5; due to the lower-energy resolution the states S_1–S_3 cannot be identified separately at that photon energy.

In order to examine the character of the surface states, the angle of incidence ϑ_i of the photon beam was varied from $\vartheta_i = 15.5°$ (mainly *s*-polarized light) to $\vartheta_i = 60°$ (strongly enhanced *p* component) at the fixed emission angle of 8.5°. For $\vartheta_i = 60°$ the emission angle was also varied slightly, showing the same behavior as found for $\vartheta_i = 45°$ (see Fig. 6). All these results are shown in Fig. 9. For S_3 no intensity dependence on ϑ_i is found, but the in-

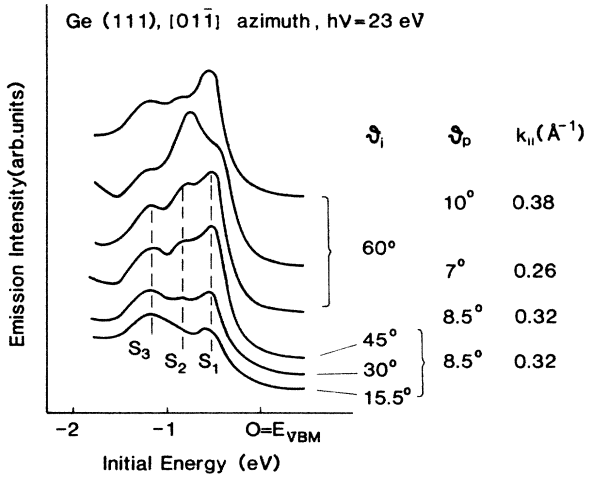

FIG. 9. Photoemission spectra recorded at a photon energy of 23 eV for various angles of incidence (ϑ_i) and emission angles (ϑ_p) as indicated.

tensity of S_1 and S_2 clearly increases roughly equally upon increasing ϑ_i. It appears then that the states S_1 and S_2 have p_z character and can be related to dangling bonds, while the state S_3 has $p_{x,y}$-like character. This is in agreement with the results of Himpsel *et al.*,[2] who found p_z-like character for S_2 and $p_{x,y}$-like character for S_3, both at the zone center.

C. Measurements along a $\langle 11\bar{2}\rangle$ azimuth

Measurements were also performed along the $\langle 11\bar{2}\rangle$ azimuth with a photon energy of 23 eV. A series of relevant spectra is shown in Fig. 10. Again, the two features A and B can be assigned to bulk-band transitions. The feature C, which we believe to be related to the surface structure, is present at the binding energy of 3.4 eV and shows no dispersion. Three surface states, S_1, S_2, and S_3, can be separately resolved around $k_{\parallel}=0.3$ Å^{-1}. The state S_1 can be followed from Γ almost to the surface Brillouin-zone boundary at $M_{1\times1}$ but the intensity of this state is rather weak. This causes some uncertainty in the designation of the peaks in the spectra taken around $M_{1\times1}$. For instance, in the spectrum at $\vartheta_p=26°$ in Fig. 10, it is not clear whether the strong peak at 0.8 eV binding energy should be assigned to S_1, or may be due to the reappearance of S_2, especially since some hint of a feature at lower binding energy can be seen. The resulting dispersions are collected in Fig. 11. No sign is found of a strongly dispersing state S_4 such as witnessed along the $\langle 01\bar{1}\rangle$ direction, although the intensity of S_3 increases strongly near the $M_{1\times1}$ point. The same difference between both azimuths was found by Nicholls *et al.* with photon energies around 10 eV.[7]

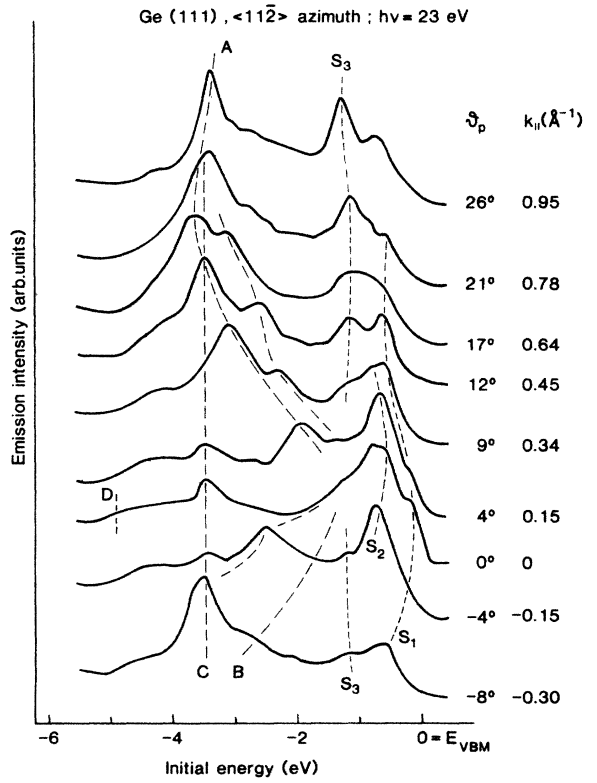

FIG. 10. Photoemission spectra recorded at a photon energy of 23 eV for various emission angles along a $\langle 11\bar{2}\rangle$ direction. Dashed lines serve as a guide to the eye. Values for $k_{\parallel}$ are calculated for a binding energy of 1 eV.

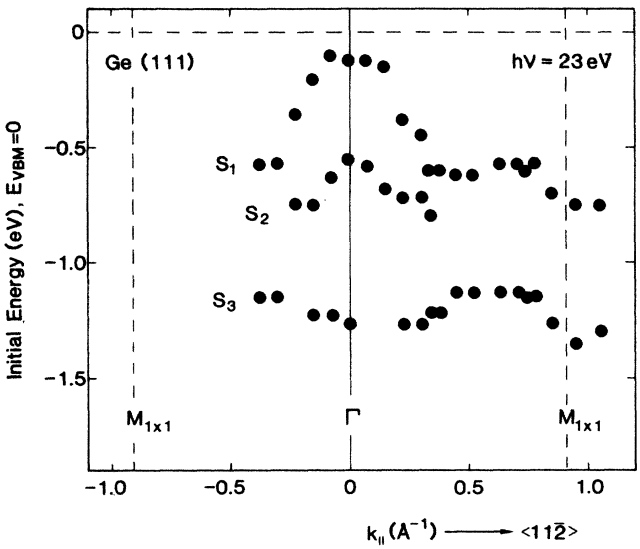

FIG. 11. Energy dispersions for the structures S_1–S_3 of Fig. 10.

IV. DISCUSSION

For Ge(111)-$c(2\times8)$ the surface structure is not as well known as for Si(111)-(7×7), but from STM measurements[5] it appears that a partial layer of adatoms is present, as in the case of Si(111); this is in accordance with the observation from Ge 3*d* core-level measurements that a fraction [about $\frac{1}{4}$ monolayer (ML)] of Ge atoms show a large change in binding energy.[17] Using this fact, models for the surface structure have been proposed, of which two are of current interest. One is an ordered adatom structure, where the adatoms are in an arrangement as suggested by Yang and Jona.[18] The other is the dimer chain model proposed by Takayanagi and Tanishiro.[19] No band-structure calculations have been reported for these models, but the local bonding geometry of the adatoms is very similar in both, and also similar to the adatom geometry in the commonly accepted dimer–adatom–stacking-fault model of Takayanagi *et al.*[20] for Si(111)-(7×7). In this geometry the adatom rests in the threefold-symmetric site above the second full layer (T_4 structure) or (inequivalently) above the fourth full layer (H_3 structure). The adatom binds to three atoms in the first layer, thereby satisfying their dangling bonds. The nearest equivalent site for an adatom must then remain empty, and this can lead to subunits of a (2×2) unit cell. Such a subunit contains one atom of the first layer which still has a dangling bond. This atom is called the rest atom. For the electronic structure of the adatom geometry (not including rest atoms) band-structure calcu-

lations based on 2×2 entities were performed in the case of Si by Northrup.[6] Also, when amounts of $\frac{1}{3}$ ML of elements M such as Al, Ga, or In are deposited, the ensuing Si(111)-$\sqrt{3}\times\sqrt{3}$:M phase is attributed to the same threefold-symmetric sites.[21] Calculations were performed for such cases[22,23] and show essentially the same behavior.

We shall start the discussion of the results on Ge guided by these calculations, which find the presence of two bands, one at about the Fermi energy and one around 2 eV binding energy. The clearest description of the behavior of this latter band was given in Ref. 23, based on calculation made for Si(111)-$\sqrt{3}\times\sqrt{3}$:In. This behavior is sketched in Fig. 12. For the $\langle 01\bar{1}\rangle$ azimuth the most outstanding features are that the band splits up, going from Γ to $K_{1\times1}$, with the largest splitting of about 0.5 eV around 0.5 Å^{-1} and that the highest intensity in photoemission is expected for the branch with highest initial energy between $\frac{1}{2}\Gamma K_{1\times1}$ and $K_{1\times1}$, but for the lowest branch beyond $K_{1\times1}$. The dispersion of the intense part of the band is therefore about 0.5 eV. For the $\langle 11\bar{2}\rangle$ azimuth the behavior is different. Going from Γ to $M_{1\times1}$ the bands show only a small splitting and cross at about $0.6\Gamma M_{1\times1}$. The splitting then becomes larger and reaches a maximum at $M_{1\times1}$ of about 0.4 eV. The dispersion of the intense part of the bands is only 0.2 eV. Before comparing this behavior with the experiments, it should be noted that it is not clear whether the adatom structure on the Ge(111) surface is centered on the T_4 or on H_3 sites. However, the difference in band structure for the two geometries is smaller than can be resolved with photoemission.[23] It should also be noted that the lattice parameters, and therefore the Brillouin-zone widths, of Si and Ge differ by no more than 4%.

The comparison makes it clear that the state S_4 found for the $\langle 01\bar{1}\rangle$ azimuth may well be derived from the adatom geometry. It appears at about $\frac{1}{2}\Gamma K_{1\times1}$, disperses 0.5 eV downward to $K_{1\times1}$, and then becomes flat. In the same picture, the state S_3 centered around the Γ point can also be ascribed to the adatom geometry as a superposition of the split bands. The calculations also show that around the $K_{1\times1}$ point the two states which we call S_3 and S_4 are again superimposed. For the $\langle 11\bar{2}\rangle$ azimuth the strongly dispersing state S_4 is not observed, in accordance with the calculations, but the state called S_3 may well be a superposition of the two upward-dispersing weak states near Γ. Near $M_{1\times1}$ it is then the downward-dispersing intense branch.

The first conclusion is, therefore, that the states S_3 and S_4 appear to be due to adatom complexes. Less clear is the situation in the case of S_1; for this we have to turn to the full unit cell. The calculations of Northrup for Si show the presence of a partly filled band which determines the Fermi energy. The filling factor for this band is determined by the relative amount of adatoms (twelve) and rest atoms (six). Charge transfer fills the rest-atom dangling-bond states so that the adatom dangling-bond states are left partly filled. This leads to the metallic surface state seen in the experiments.[24] In the ordered adatom model for Ge(111) there are four adatoms and four rest atoms. Charge transfer then leads to empty adatom states and the state S_1 would not be expected. In the dimer chain model there are no rest atoms so that the adatom dangling bonds remain. Again this would not lead to a filled state S_1. It should be remembered, however, that experiments are always performed on surfaces containing three different $c(2\times8)$ domains and therefore also domain walls, which may have different numbers of adatoms and rest atoms, leading to a different charge distribution. Calculations based on a correct atomic structure are needed to resolve this issue.

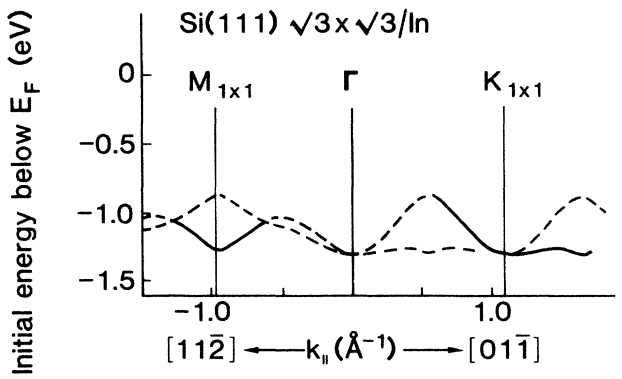

FIG. 12. Energy dispersions as calculated for Si(111)-$\sqrt{3}\times\sqrt{3}$:In (from Ref. 23). Dashed lines indicate low emission, solid lines indicate strong emission.

This leaves discussion of the state S_2. This state is found on both the Ge(111)-$c(2\times8)$ surface (binding energy around 0.8 eV) and on the Si(111)-(7×7) surface (binding energy around 1 eV) and is not due to the adatom geometry. It has the character of a dangling-bond state and STM measurements on Si (Ref. 1) showed that it derives from the rest atoms. It seems probable that it then also derives from the rest atoms in the case of Ge. The ordered adatom structure contains rest atoms, but the dimer chain model does not, so that the former model appears to be more likely. Finally, we want to remark that the dispersions of the states S_1 and S_2 found in our experiments indicate the possibility of hybridization between these states. The similar character might lead to a repulsion of energy bands which would have crossed (around 0.3 Å^{-1}) without the presence of hybridization.

V. SUMMARY

Summarizing our results, we have used angularly resolved photoemission measurements and molecular-beam epitaxy in order to study the $c(2\times8)$ reconstruction on the Ge(111) surface. On carefully prepared surfaces, four surface states can be found along the $\langle 01\bar{1}\rangle$ azimuth for a range of photon energies. Along the $\langle 11\bar{2}\rangle$ azimuth three different structures are found, which may actually represent the same four states with different dispersions and relative intensities. It is argued that two of these states, S_3 and S_4, are due to adatom structures on the Ge(111) surface, very similar to adatom

geometries on the Si(111)-(7×7) surface. The state S_1 cannot yet be fully explained by the existing structural models. The state S_2 is possibly due to rest atom dangling-bond states, so that the measurements show some preference for the ordered adatom model over the dimer chain model.

ACKNOWLEDGMENTS

Thanks are due to W. Gerits, for technical assistance prior to the measurements, and to the technical staff of LURE for their help during our stay.

[1]R. J. Hamers, R. M. Tromp, and J. E. Demuth, Phys. Rev. Lett. **56**, 1972 (1986).
[2]F. J. Himpsel, D. E. Eastman, P. Heimann, B. Reihl, C. W. White, and D. M. Zehner, Phys. Rev. B **24**, 1120 (1981).
[3]T. Yokotsuka, S. Kono, S. Suzuki, and T. Sagawa, J. Phys. Soc. Jpn. **53**, 696 (1984).
[4]R. D. Bringans, R. I. G. Uhrberg, R. Z. Bachrach, and J. E. Northrup, J. Vac. Sci. Technol A **4**, 1380 (1986).
[5]R. S. Becker, J. A. Golovchenko, and B. S. Swartzentruber, Phys. Rev. Lett. **54**, 2678 (1985).
[6]J. E. Northrup, Phys. Rev. Lett. **57**, 154 (1986).
[7]J. M. Nicholls, G. V. Hansson, R. I. G. Uhrberg, and S. A. Flodström, Phys. Rev. B **33**, 5555 (1986).
[8]P. K. Larsen, W. A. M. van Bers, J. M. Bizau, F. Wuillemier, S. Krummacher, V. Schmidt, and D. Ederer, Nucl. Instrum. Methods **195**, 245 (1982).
[9]J. L. Wiza, Nucl. Instrum. Methods **162**, 587 (1979).
[10]A. A. MacDowell, I. H. Hillier, and J. B. West, J. Phys. E **16**, 487 (1983).
[11]E. A. Kraut, R. W. Grant, J. R. Waldrop, and S. P. Kowalczyk, Phys. Rev. B **28**, 1965 (1983).
[12]R. J. Phaneuf and M. B. Webb, Surf. Sci. **164**, 167 (1985); see also D. J. Chadi and C. Chiang, Phys. Rev. B **23**, 1843 (1981).
[13]R. D. Bringans and H. Höchst, Phys. Rev. B **25**, 1081 (1982).
[14]A. L. Wachs, T. Miller, T. C. Hsieh, A. P. Shapine, and T. C. Chiang, Phys. Rev. B **32**, 2326 (1985).
[15]J. M. Nicholls, G. V. Hansson, U. G. Karlsson, P. E. S. Persson, R. I. G. Uhrberg, R. Engelhardt, S. A. Flodström, and E.-E. Koch, Phys. Rev. B **32**, 6663 (1985).
[16]J. Aarts, A.-J. Hoeven, and P. K. Larsen (unpublished).
[17]S. B. DiCenzo, P. A. Bennet, D. Tribula, P. Thiry, G. K. Wertheim, and J. E. Rowe, Phys. Rev. B **31**, 2330 (1985).
[18]W. S. Yang and F. Jona, Phys. Rev. B **29**, 899 (1984).
[19]K. Takayanagi and Y. Tanishiro, Phys. Rev. B **34**, 1034 (1986).
[20]K. Takayanagi, Y. Tanishiro, M. Takahashi, and S. Takahashi, J. Vac. Sci. Technol. A **3**, 1502 (1985).
[21]T. Kinoshita, S. Kono, and T. Sagawa, Phys. Rev. B **34**, 3011 (1986).
[22]J. E. Northrup, Phys. Rev. Lett. **53**, 683 (1984).
[23]J. M. Nicholls, P. Mårtensson, G. V. Hansson, and J. E. Northrup, Phys. Rev. B **32**, 1333 (1985).
[24]D. E. Eastman, J. Vac. Sci. Technol. **17**, 492 (1980).

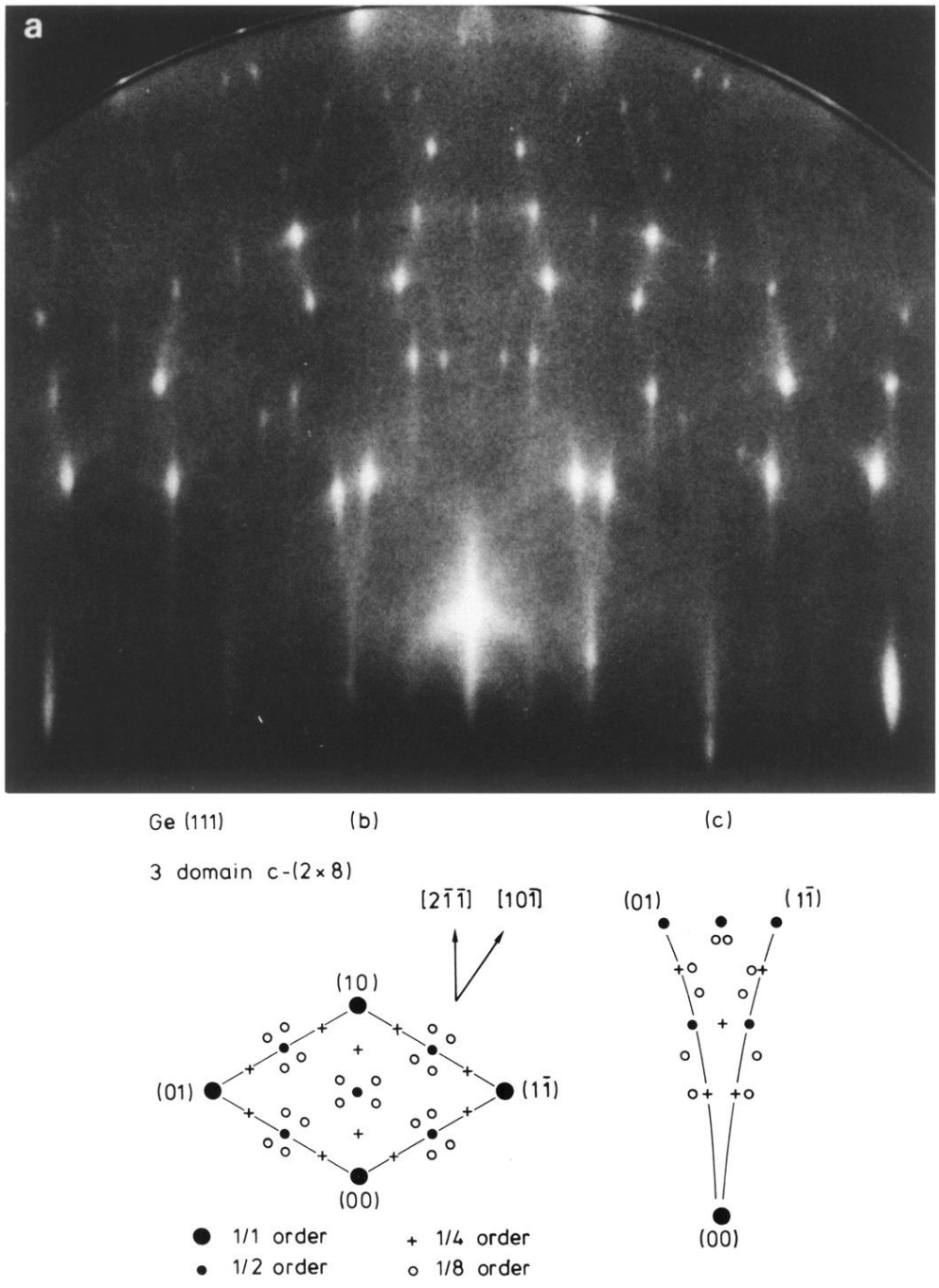

FIG. 1. (a) RHEED pattern of the three-domain $c(2\times8)$ reconstruction on a clean Ge(111) surface along a $\langle\bar{2}11\rangle$ azimuth. The electron-beam energy is 12 keV and the angle of incidence with respect to the surface plane 2.5°. (b) Reciprocal mesh for the three domains of the $c(2\times8)$ unit cell. (c) Elongation of the lower half of the pattern shown in (b) due to the RHEED geometry.